


RESEARCH ARTICLE | APRIL 03 2025

# Determining the optimum reference orbits using Lagrange's series for geocentric satellite in low earth orbit

Rasha H. Ibrahim 

*AIP Conf. Proc.* 3282, 050013 (2025)

<https://doi.org/10.1063/5.0264851>



## Articles You May Be Interested In

Is coverage a factor in non-gaussianity of imf parameters?

*AIP Conf. Proc.* (July 1996)


National space navigation over the past two decades of the 21st century. Positive look

*AIP Conf. Proc.* (November 2019)


Aircraft animation and air route tracing simulation system

*AIP Conf. Proc.* (March 2020)


03 April 2025 23:50:02




Nanotechnology & Materials Science




Optics & Photonics



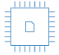
Impedance Analysis




Scanning Probe Microscopy



Sensors




Failure Analysis & Semiconductors



**Unlock the Full Spectrum.**  
From DC to 8.5 GHz.  
Your Application. Measured.

[Find out more](#)



# Determining the Optimum Reference Orbits Using Lagrange's Series for Geocentric Satellite in Low Earth Orbit

Rasha H. Ibrahim<sup>1, a)</sup>

<sup>1</sup> *Department of Astronomy and Space, College of Science, University of Baghdad, Baghdad, Iraq.*

<sup>a)</sup> Corresponding author: Rasha.Ibrahim@sc.uobaghdad.edu.iq

**Abstract.** The Taylor series is defined by the f and g series. The solution to the satellite's equation of motion is expanding to generate Taylor series through the coefficients f and g. In this study, the orbit equation in a perifocal system is solved using the Taylor series, which is based on time changing. A program in matlab is designed to apply the results for a geocentric satellite in low orbit (height from perigee,  $h_p = 622$  km). The input parameters were the initial distance from perigee, the initial time, eccentricity, true anomaly, position, and finally the velocity. The output parameters were the final distance from perigee and the final time values. The results of radial distance as opposed to time were plotted for dissimilar times in seconds and their comparison with the exact solution, with the aim of selecting an optimized reference orbit at a height of 622 km. The results indicated that the two series diverged excessively as the time increased from the exact solution, excluding the time of 850 sec. The f and g series had a little shift. Besides, the root mean square error (rmse) is computed for 750 sec. It was about 5 for the two series before diverging at about 180 sec and rapidly growing with time. For 850 sec, the (rmse) is approaching 10 for the two series and increasing quickly over time. So, the (rmse) is directly proportional to time, which means that as time increases, the diverging behavior and the value of the (rmse) will also increase. If more terms ( $\Delta t$ ) are used for the two series and more time is included, the two series will deviate from the exact solution. The program's results are compared to other published studies in this field; they demonstrated high convergence.

**Keywords:** Perifocal System, Lagrange Series, True Anomaly, Taylor Series, Eccentricity, Elliptical Orbit, Dynamic Orbit.

## INTRODUCTON

Celestial objects and space phenomena can be studied in astronomy. This field uses principles of physics and numerical mathematics to describe the creation, evolution, and celestial events in space [1]. Celestial objects take account of planets, stars, clusters, and moons [2]. Significant events include x-ray bursts, background radiation [3], pulsars, supernova explosions and cosmic microwaves. Any phenomenon that emerges outside of Earth's atmosphere [4] is also studied by astronomy, including refractive index [5], atmospheric parameters besides electron density estimation [6]. In observational astronomy [7], data are collected by observations of celestial objects [8]. The main principles of remote sensing and image processing are then utilized to examine the collected data [9]. One of

the most essential fields of celestial mechanics is still dynamic orbit propagation [10]. Celestial mechanics developed the method of solving a satellite's equation of motion or that of other celestial objects without using measurements [11]. The explanation of a satellite's equation of motion is divided into four forms [12]: numerical, analytical, semi-analytical and classical [13]. The basic principle of Lagrange's method is series expansion; it simply needs one function generation for each step. The Taylor series likes single-step methods, as the order increases, stability and precision are also increased. It is a mixture of a single method and a multi-step method [14]. Various low altitude satellites are not staying in their orbits around the Earth, but are approaching it, because of the influence of the drag force on the orbiting satellites [15]. The atmosphere gradually becomes thinner at higher altitudes, making the homecoming of satellites to Earth difficult [16]. The altitude of the satellite will decrease when it approaches a denser region of the atmosphere. Resistance between the surface of the satellite and the drag force produces a significant amount of heat [17]. This comes about due to the satellite's rapid velocity. A great quantity of heat is formed, which is enough to put an end to the entire satellite or portions of it [18]. The FORMAC computer program is used to apply the two series  $f$  and  $g$  in a Keplerian gravitational field that is advanced by Sconzo et al. [19]. These two Taylor series are used to determine the orbit of the satellite, like Gauss and Lambert. In addition, the coefficients for the two and three body concerns are achieved [20]. Feng used GPS-based data; the concept of reduced dynamic orbit determination was put into practice for LEO satellites [21]. In 2003, Lin and Xin used  $f$  and  $g$  series with the Laplace method for determining the initial orbit using angular data. Sharifi and Seif developed Lagrange coefficients from  $J_2$  [22]. In 2009, Fouad and Anas studied the impact of the position on the time for astronomical twilight [23]. Pellegrini et al. used the solution to the stark problem with Sundman transformations for the Taylor series [24]. In 2019, Fouad calculated the differences for the sunrise, sunset as well as the time for the day length [25]. Astronomy is divided into two subfields: theoretical and observational [26]. Information gathering from observations of celestial objects is the goal of observational astronomy. Developing computational or analytical models to define astronomical events and celestial objects is the aim of theoretical astronomy [27]. These branches work well together; in this study, theoretical astronomy is studied in order to determine the best reference orbit [28].

## THEORY

### Perifocal System

This system is described by a body starting from the focus of the orbit, as illustrated in Figure 1a. The  $x$  axis extends from the focus and passes through the periapse, which is the nearest point to the body from the focus of the elliptical orbit. This axis is vertical on the  $y$  axis; the  $y$  axis represents the path of the body along the elliptical orbit. The true anomaly is an angle formed from the periapse as well as the  $y$  axis. The  $xy$  plane and  $z$  axis are perpendicular to each other, as shown in Figure 1b. The position vector  $\mathbf{r}$  [29]:

$$r = x\hat{\mathbf{p}} + y\hat{\mathbf{q}} \quad (1)$$

Where  $x$ : is the position relative to the  $x$  direction,  $\hat{\mathbf{p}}$ : is a vector in the  $x$  direction,  $y$ : is the position relative to the  $y$  direction,  $\hat{\mathbf{q}}$ : is a vector in  $y$  direction,  $r$ : is the magnitude of  $\mathbf{r}$  in the  $x$  and  $y$  direction and represented by [29]:

$$r = \frac{h^2}{\mu} \times \frac{1}{1 + e \cos(\theta)} \quad (2)$$

Where  $h$ : is the angular momentum,  $\mu$ : is the product of the gravitational constant with the mass of the Earth,  $e$ : is a coefficient, denotes the eccentricity of the orbit,  $\theta$ : is an angle that refers to true anomaly.

The orbit equation is another name for equation (2). As a result, it can be written in terms of the perifocal system as [11]:

$$r = \frac{h^2}{\mu} \times \frac{1}{1 + e \cos(\theta)} \times (\cos(\theta)\hat{\mathbf{p}} + \sin(\theta)\hat{\mathbf{q}}) \quad (3)$$

By taking the time derivative of equation (1), one can calculate the velocity as follow [29]:

$$v = v_x\hat{\mathbf{p}} + v_y\hat{\mathbf{q}} \quad (4)$$

Here,  $v_x = -\frac{\mu}{h} \sin(\theta)$  and  $v_y = \frac{\mu}{h} \times (e + \cos(\theta))$  Hence, equation (4) can be written in terms of perifocal system as [29]:

$$v = \frac{\mu}{h} [-\sin \theta \hat{p} + (e + \cos \theta) \hat{q}] \quad (5)$$

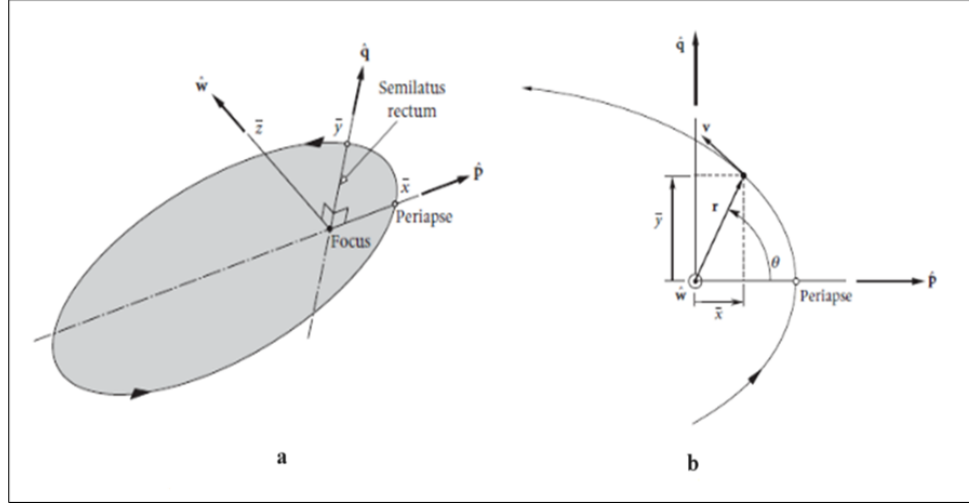


FIGURE 1. The Perifocal System

### The $f$ and $g$ Series

This series is employed as a classical method used in celestial mechanics for determining celestial body orbits based on the Keplerian motion of satellites [14]. It is used to describe the relationship between the changing of a true anomaly and time; the objective of this relation is to find the position and velocity with respect to time. Polynomial equations for  $f$  and  $g$  are developed in order to replace the changing of time for a true anomaly since times are close to the initial time. The following describes the Taylor series [29]:

$$r(t) = \sum_{n=0}^{\infty} \frac{1}{n!} r^{(n)}(t_0) (t - t_0)^n \quad (6)$$

Where  $t_0$ : is the time at the initial point,  $t$ : is the time at the final point,  $r^{(n)}(t_0)$ : is the distance at initial time for  $n^{\text{th}}$  the time derivative and is calculated as follows [29]:

$$r^{(n)}(t_0) = \left( \frac{d^n r}{dt^n} \right)_{t=t_0} \quad (7)$$

So, the  $f$  and  $g$  series in terms of the change in time are [29]:

$$f = 1 - \frac{\mu}{2r_0^3} \Delta t^2 + \frac{\mu}{2} \frac{r_0 \cdot v_0}{r_0^5} \Delta t^3 + \frac{\mu}{24} \left[ 2 \frac{\mu}{2r_0^6} + \frac{v_0^2}{r_0^5} - 15 \frac{(r_0 \cdot v_0)^2}{r_0^7} \right] \Delta t^4 \quad (8)$$

$$g = \Delta t - \frac{\mu}{6r_0^3} \Delta t^3 + \frac{\mu}{4} \frac{(r_0 \cdot v_0)}{r_0^5} \Delta t^4 \quad (9)$$

Where  $r_0$ : is the initial distance at  $t_0$ ,  $v_0$ : is the initial velocity at  $t_0$ ,  $\Delta t$ : is the difference in time between the point at final time and the point at initial time.

## CALCULATIONS

### Calculation of the Radial Distance

The flowchart below is required to create the program and complete the requirements of the study.

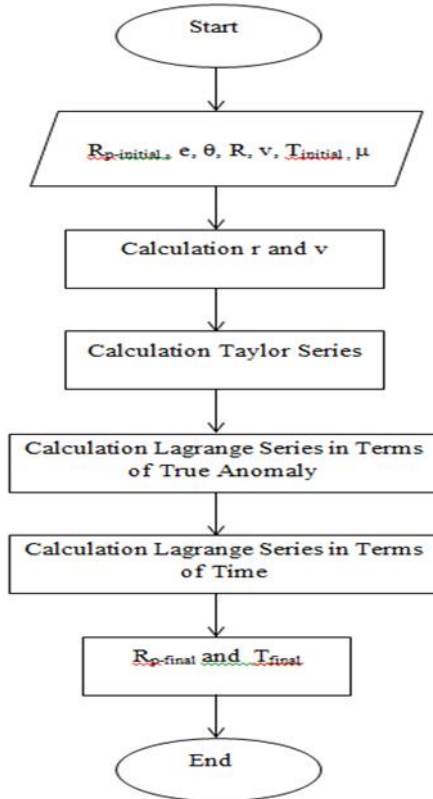


FIGURE 2. The program to calculate the radial distance

### Calculation of the Root Mean Square Error (RMSE) for the Radial Distance

The reference position of the satellite is based on the reference orbit; both are different from the actual position of the satellite. The disparity between the square of these two positions  $r_i$  and  $r_{Exact}$  over number of measurements is known as the (rmse). To reduce this value, the reference orbit is calculated as close as possible with respect to the actual orbit. The reference orbit is different from the actual orbit for two reasons: firstly, making use of incorrect started value settings; and secondly, imprecise modeling of perturbations acting on a satellite, the (rmse) is calculated by [24]:

$$rmse = \sqrt{\frac{\sum_i (r_i - r_{Exact})^2}{R}} \quad (10)$$

Where,  $r_i$  is the value due to the f and g series of the  $i^{th}$ ,  $r_{Exact}$  is the exact value measured from [36], and R is the number of measurements.

## RESULTS AND DISCUSSION

In this paper, the results are applied to a geocentric satellite in low orbit with a height from perigee ( $h_p$ ) of 622 km. The eccentricity of the orbit and the perigee radius were 0.1 and 7000 km respectively. The radial distance is plotted against time using the f and g. As seen in Figure 3, the solution by the f series diverges from the exact solution, whereas the solution by the g series is more divergent as compared with f. After roughly 390 sec in Figure 3, the f series begins to deviate significantly from the exact solution, but the g series is deviated after around 280 sec. Figure 4 shows that the radial distance for the f series increases from 7000 km to 8600 km and intersects with the ideal solution at time 850, while the radial distance for the g series has a value between (7000-7890) km. This leads to a stable orbit as compared with the exact solution. In Figure 5, the f series begins to shift further towards the y-axis and intersect with the exact solution at 1200 sec, while the g series diverges more from the exact solution with a little hump at 900 sec. When the time is increased to 1050 sec, the two series will disagree with the exact. The two series in Figure 6 deviate more from the exact solution as the time increases to 1150 sec. The f and g series will deviate more and more from the exact solution as more time is spent calculating the radial distance. If more terms ( $\Delta t$ ) are included for equations (8 and 9) and more time is used, the two series will deviate from the exact solution, as seen in Figure 7. As a result, the radial distance of convergence is measured at this moment and has a value of 1550 sec, while Bond and Allman found that this value equals 1700 sec [29]. Additionally, the (rmse) in this study is computed for 750 sec. It was about 5 for the two series before diverging at about 180 sec and rapidly growing with time. For 850 sec the (rmse) is approaching 10 for the two series and increasing quickly over time. So, the (rmse) is directly proportional to time, which means that as time increases, the diverging behavior and the value of the (rmse) will also increase. The program's results are compared to [29,31], they demonstrated high convergence

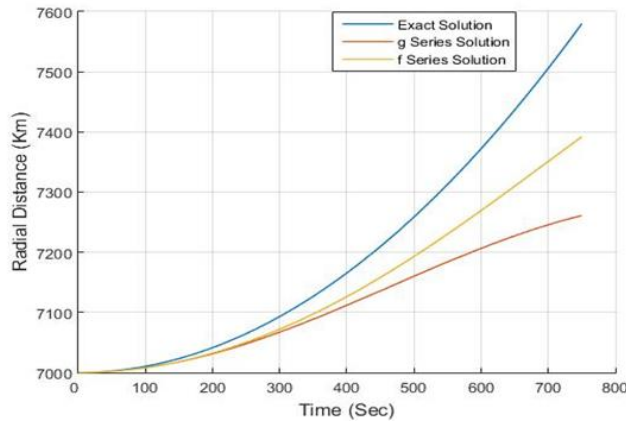


FIGURE 3. Plot the radial distance against time for 750 sec

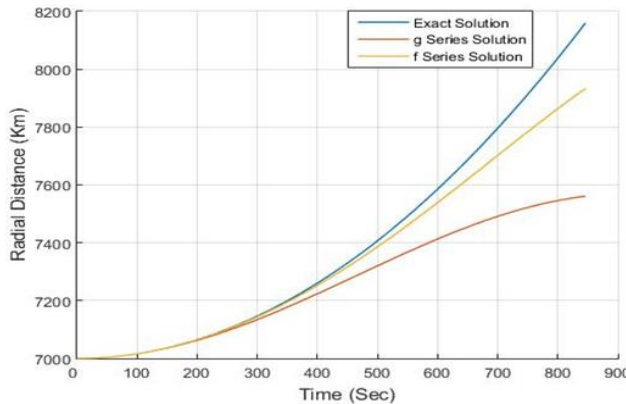
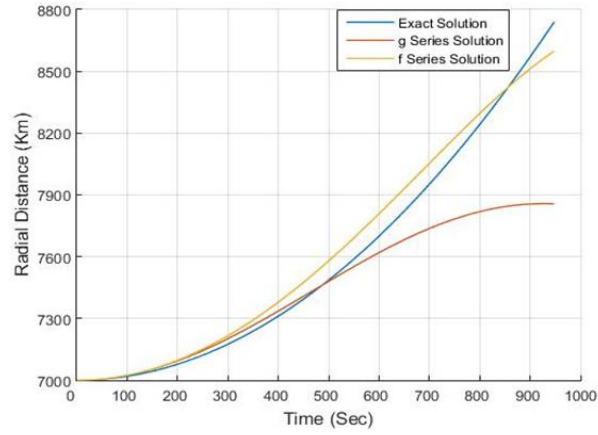
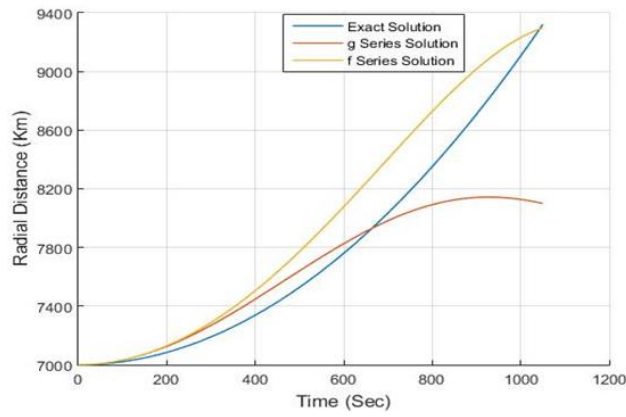


FIGURE 4. Plot the radial distance against time for 850 sec



**FIGURE 5.** Plot the radial distance against time for 950 sec



**FIGURE 6.** Plot the radial distance against time for 1050 sec

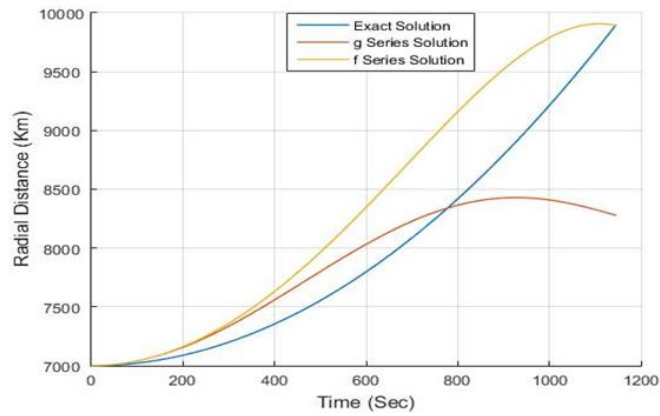


**FIGURE 7.** Plot the radial distance against time for 1150 sec

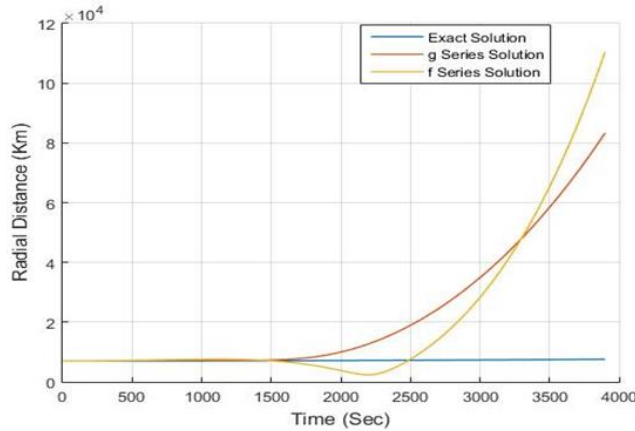


**FIGURE 8.** Plot the radial distance against time for 4000 sec

## CONCLUSION

This research could lead to the following conclusions:

1. When the time is less than or equal to 850 sec, the f and g series begin to diverge from the exact solution and exhibit a tendency to the x-axis. As time exceeds 850 sec and reaches 1150 sec, the two series begin to deviate from the exact solution and exhibit a tendency toward the y-axis.
2. If the g and f series are calculated over an extended period of time, the result of the solution will agree with the actual solution at a specific time. After a certain period of time, the g and f series will deviate from the actual solution. This demonstrates that Lagrange series is only valid for a short time.
3. The time of 850 sec is more appropriate for the exact solution, particularly for the f series.
4. The (rmse) is calculated for 750 sec. It was about 5 for the two series before diverging at about 180 sec and rapidly growing with time. For 850 sec the root mean square error is approaching 10 for the two series and increasing quickly over time. So, the (rmse) is directly proportional to time, which means that as time increases, the diverging behavior and the value of the (rmse) will also increase.
5. If more terms ( $\Delta t$ ) are used for the two series and more time is included, the two series will deviate from the exact solution. In addition, a future work is planned to use the Taylor series (the f and g series) in order to find the velocity in terms of true anomaly or time. Also, more orders are used with equations (8 and 9).

## ACKNOWLEDGMENTS

I'd like to thank the chief of the Department of Astronomy and Space, academic staff, colleagues, and all friends at the College of Science, University of Baghdad, for their significant guidance and support.

## REFERENCES

1. . U.E.Jallod, H.S.Mahdi, and K.M.Abood, Simulation of Small Radio Telescope Antenna Parameters at Frequency of 1.42 GHz. *Iraqi Journal of Physics*. 20 (1)37- 47 (2022).
2. H.S.Ali, Performance Estimation of Solar Imagery Using Different Types of Atmospheric Turbulence Models V. *Iraqi Journal of Science*. 64 (7) 3679-3690 (2023).
3. M. N.Al Najm, O. L. Polikarpova, Yu. A. Shchekinov, "Ionized Gas in the Circumgalactic Vicinity of the M81 Galaxy Group. *Astronomy Reports*. 60(4)389–396 (2016).
4. M.F.Hassan, and W.I.Yaseen, Electron Density Estimation by Electrostatic Probe for Plasma Generated Near the Spacecraft Returning to the Earth's Atmosphere. *Iraqi Journal of Science*. 64(6)3194- 3204 (2023).
5. W.I.Yaseen, C.B.Yasser, and N.A.Mohammed, Calculation of the Parameters for Atmospheric Model for the Earth. *Al-Nahrain Journal of Science*. 12(3) 64-69 (2009).



6. R.N.Hassan, and H.S.Ali, Performance Estimation and System Modeling for Refractive Index Structure Constant Cn2. *Karbala International Journal of Modern Science*. 9(2) 178 - 186 (2023).
7. Uday E. Jallod, Kamal M. Abood; Characteristics measurement of Baghdad University radio telescope for hydrogen emission line. *AIP Conf. Proc.* 11 December 2019; 2190 (1): 020035. <https://doi.org/10.1063/1.5138521>.
8. A. H. Abdullah, Pavel Kroupa, Patrick Lieberz and Rosa Amelia González-Lópezlira , On the primordial specific frequency of globular clusters in dwarf and giant elliptical galaxies. *Astrophysics and Space Science*. 364(86)2019.
9. M.A.Hameed, S.B.Al-Khoja, and R.R.Ismail, Small Binary Codebook design depending on Rotating Blocks. *Iraqi Journal of Science*. 62(10)3719-3723(2021).
10. W.Ulrich, *Astronautics: The Physics of Space Flight*, third ed., Springer, 2019, pp. 115-120.
11. G.Seeber, *Satellite Geodesy*, second ed., Berlin Walter de Gruyter, 2003, pp. 80-90.
12. H.B.Richard, *An Introduction to the Mathematics and Methods of Astrodynamics*, Revised ed., AIAA Education Series,1999, pp.77-80.
13. R.H.Ibrahim, and A.H.Saleh, Finding the Exact Solution of Kepler's Equation for an Elliptical Satellite Orbit Using the First Kind Bessel Function, *Iraqi Journal of Science*. 65 (2) 1129-1137 (2024).
14. M.R.Seif, The generalized F and G series for the satellite orbit propagation. *Earth Observation and Geomatics Engineering*. 1(2)71 - 81 (2017).
15. J.N.Pelton, chapter 2: Orbits, Services and System, *Satellite Communication*, Springer, Briefs in Space Development, 2012, pp.5 - 17.
16. R.Bate,D.Mueller, and J.White, *Fundamental of Astrodynamics*,Dover publications,Inc.NewYork,1971, p.77-78.
17. P.P.Dabeer, and S.B.ManeDeshmukh, Lagrangian Mechanics Application for Determination of Reentry Rate of Low Earth Orbiting Satellite. *International Journal of Current Engineering and Technology*. 6(5) 1 - 4 (2016).
18. C.W.Robert, *Satellite Basics for Everyone*, i Universe, Inc. Bloomington, 2012, p.100-103.
19. P.Sconzo,A.LeSchack, and R.Tobey, Symbolic computation of F and G series by computer, *Astronomical Journal*. (70) 269-275 (1965)
20. J.Bem, and B.Szczodrowska-Kozar, High order F and G power series for orbit determination, *Astronomy and Astrophysics Supplement*. (110) 411-417(1995).
21. Y.Feng, An Alternative Orbit Integration Algorithm for GPS-Based Precise LEO Autonomous Navigation. *GPS Solutions*. 5(2) 1-11 (2001).
22. L.Lin, and W.Xin, A method of orbit computation taking into account the earth's oblateness. *Chinese Astronomy and Astrophysics*. 27(3) 335 - 339 (2003).
23. A.M.Fouad, and T.S.Anas, Study the effect of position on the time of astronomical twilight. *Baghdad Science Journal*. 6 (4) (2009) 797-803.
24. E.pellegrini, R.Russell, and V.Vittaldev, F and G Taylor series solutions to the Stark and Kepler problems with Sundman transformations, *Celestial Mechanics and Dynamical Astronomy*. (118) 355 -378 (2014).
25. K.Hannu, K.Pekka, O.Heikki, P.Markku, and J.D.Karl, *Fundamental Astronomy*, sixth ed., Springer Berlin Heidelberg, New York, 2017, p. 505-555.
26. P.Delia, and V.Alex, *Cosmology for the Curious*, second ed., Springer, 201, p.72-100.
27. M.Zechmeister, CORDIC-Like Method for Solving Kepler's Equation. *Astronomy and Astrophysics*. 619(A128) 1 - 9 (2018)
28. D.C.Howard, *Orbital Mechanics for Engineering Students*. third ed., Elsevier Aerospace Engineering Series, 2010, p.220-225.
29. O.Montenbruck, *Numerical Integration Methods for Orbital Motion*. *Celestial Mechanics and Dynamical Astronomy*. (53) 59-69 (1992).
30. O.Montenbruck, and E.Gill, *Satellite Orbits Models Methods and Applications*. second ed., Springer-Verlag Berlin Heidelberg, Germany, 2001, p.55-60.